Mon. Not. R. Astron. Soc. **350,** 1437–1444 (2004) doi:10.1111/j.1365-2966.2004.07739.x

Equilibria of a self-gravitating, rotating disc around a magnetized compact object

J. Ghanbari⋆ and S. Abbassi⋆

Department of Physics, School of Sciences, Ferdowsi University of Mashhad, Mashhad 91775-1436, Iran

Accepted 2004 February 16. Received 2004 February 16; in original form 2004 January 16

ABSTRACT

We examine the effect of self-gravity in a rotating thick-disc equilibrium in the presence of a dipolar magnetic field. First, we find a self-similar solution for non-self-gravitating discs. The solution that we have found shows that the pressure and density equilibrium profiles are strongly modified by a self-consistent toroidal magnetic field. We introduce three dimensionless variables, C_B, C_c and C_t, which indicate the relative importance of toroidal component of the magnetic field (C_B), and centrifugal (C_c) and thermal (C_t) energy with respect to the gravitational potential energy of the central object. We study the effect of each of these on the structure of the disc. Secondly, we investigate the effect of self-gravity on the discs; thus, we introduce another dimensionless variable (C_g) which shows the importance of self-gravity. We find a self-similar solution for the equations of the system. Our solution shows that the structure of the disc is modified by the self-gravitation of the disc, the magnetic field of the central object and the azimuthal velocity of the gas disc. We find that self-gravity and magnetism from the central object can change the thickness and the shape of the disc. We show that as the effect of self-gravity increases the disc becomes thinner. We also show that, for different values of the star's magnetic field and of the disc's azimuthal velocity, the disc's shape and its density and pressure profiles are strongly modified.

Key words: accretion, accretion discs – black hole physics – MHD – galaxies: active.

1 INTRODUCTION

The theory of accretion discs, motivated to a large degree by their occurrence in some binary systems, particularly cataclysmic variables, has been most fully developed for the thin Keplerian discs (Pringle 1981). Based on their geometric shapes, accretion discs are generally divided into two distinct classes: thin discs and thick discs. The theory of thin accretion discs (Shakura & Sunyaev 1973) is well understood, whereas there is no universally accepted model for thick accretion discs. The current interest in this theory is due to the possibility that thick discs may be relevant to the understanding of central power sources in radio galaxies and quasars. Observational evidence suggests that, in the centre of many galaxies, matter is somehow ejected to large distances and gives off high-energy radiation as it interacts with the external medium. There are other theoretical reasons for pursuing the study of thick discs. In the theory of thin discs, radial pressure gradients are neglected and vertical pressure balance is solved separately. It has been shown that this approximation is valid as long as the disc is geometrically thin. This condition may be violated in the innermost region of accretion discs around stellar black holes and neutron stars. The study of thick discs provides a better theoretical understanding of thin discs as a limiting case and enables us to deal with intermediate situations (Frank, King & Raine 1992).

When considering the formation process of astrophysical objects, such as galaxies and stars, the most crucial factor is self-gravity. In the standard thin accretion disc model, the effect of self-gravity is neglected, and only pressure supports the vertical structure. By contrast, the theory of self-gravitating accretion discs is less developed. Early numerical work of self-gravitating accretion discs began with *N*-body modelling (Cassen & Moosman 1981; Tomley, Cassen & Steiman-Cameron 1991). The time evolution of a non-self-gravitating viscous disc has long been studied, and now we have a good theory describing its steady structure and its basic time-dependent behaviour (Shakura & Sunyaev 1973; Lynden-Bell & Pringle 1974). However, with the added assumption of self-gravity in the disc, it is not easy to follow its dynamical evolution, mainly because the basic equations for the discs are highly non-linear (e.g. Paczynski 1978; Fukue & Sakamoto 1992). To solve the non-linear equations of self-gravitating discs, the technique of self-similar analysis is sometimes useful. Several classes of self-similar solutions were known previously, but all of them considered a disc in a fixed, external potential. Self-similar behaviour provides an important class of solutions to the self-gravitating fluid equations. On the one hand, many physical problems often attain self-similar limits

⋆E-mail: ghanbari@ferdowsi.um.ac.ir (JG); abasi@wali.um.ac.ir (SA)

for a wide range of initial conditions. On the other hand, the self-similar properties allow us to investigate properties of solutions in arbitrary details, without any of the associated difficulties of numerical hydrodynamics.

Pen (1994) presented a general classification of self-similar self-gravitating fluids. Fukue & Sakamoto (1992) also analysed the vertical structure of self-gravitating discs, but it is impossible to compare their models with realistic discs, because they computed the vertical structure using the thin-disc approximations for polytropes. Finally, using the numerically method proposed by Hachisu (1986a,b) and Hashimoto, Tohline & Eriguchi (1987), Woodward et al. (1992) developed a code to investigate the interaction between a disc and its central object. However, they only considered polytropic discs. Hashimoto, Eriguchi & Muller (1995) presented a two-dimensional equilibrium model for self-gravitating Keplerian discs. They showed that the shape of the disc (or disc thickness) is flounced by the rotational law and the ratio of the disc mass to the mass of the central star. Bodo & Curir (1992) computed the equilibrium structure of a self-gravitating thick accretion disc by an iterative procedure which produced a final density distribution in equilibrium with the potential coming from it. They showed that the geometrical size and shape of the discs are influenced by self-gravity of the disc.

Accretion discs, containing magnetic fields, have been the subject of intense study in recent years. The role of the magnetic field in the equilibrium of accretion discs has been investigated by some authors (Blandford & Znajek 1977; Lubow et al. 1994) for thin-disc models. An ideal magnetohydrodynamics (MHD) equilibrium with azimuthal velocity and poloidal magnetic field has been analysed (Lovelace et al. 1986; Mobarry & Lovelace 1986). Using numerical methods, these authors found that the magnetic field may change the shape and angular momentum distribution in the disc. Thick-disc configurations with a poloidal magnetic field have been studied by Tripathy, Prasanna & Das (1990) in the MHD framework (Banerjee et al. 1995). They investigated the equilibrium structure of thick discs and their stability in the presence of a dipolar magnetic field due to a non-rotating central object. Their solution shows that the pressure and the density equilibrium profiles are strongly modified by a toroidal magnetic field, resulting from the interaction between the permanent dipolar magnetic field and the inertia of the gas disc. In a magnetized disc, the inertia of the gas is expected to bend the magnetic field lines backwards, creating a toroidal component, which in turn may collimate a hydrodynamic outflow over long distances, forming jets. They assumed that the disc is non-accreting, stationary, axisymmetric, non-viscous, magnetized, and that it is in equilibrium around a compact object, with only an azimuthal motion V_ϕ.

We are interested in analysing the role of self-gravity in thick-disc equilibrium in the presence of the dipolar magnetic field of a central star. The outline of this paper is as follows. The general formalism of the problem is discussed in Section 2. A self-similar solution of the equilibrium of non-self-gravitating accretion discs in the presence of a dipolar magnetic field is constructed in Section 3. A self-similar solution of self-gravitating magnetized accretion discs is constructed in Section 4 and a summary of the main ideas is given in Section 5.

2 GENERAL FORMALISM

As stated in the introduction, we are interested in analysing the role of self-gravity in a thick-disc equilibrium in the presence of the dipolar magnetic field of a central star. For simplicity, we ignore the influence of energy dissipation. We consider the disc as a non-accreting MHD flow around a magnetized, non-rotating, central compact object. The disc is assumed to be stationary and axisymmetric. We use a spherical polar, inertial, coordinate system, (r, θ, ϕ), with the origin fixed on the central object. The basic equations are two components of the Euler equation in the (r, θ) direction and the Poisson equation:

$$\frac{\partial \Psi}{\partial r} = -\frac{1}{4\pi r}\frac{B_\phi}{\rho}\frac{\partial}{\partial r}(rB_\phi) - \frac{GM}{r^2} - \frac{1}{\rho}\frac{\partial p}{\partial r} + \frac{V_\phi^2}{r}, \tag{1}$$

$$\frac{\partial \Psi}{\partial \theta} = -\frac{1}{4\pi \sin\theta}\frac{B_\phi}{\rho}\frac{\partial}{\partial \theta}(B_\phi \sin\theta) - \frac{1}{\rho}\frac{\partial p}{\partial \theta} + V_\phi^2 \cot\theta, \tag{2}$$

$$\frac{1}{r^2}\frac{\partial}{\partial r}\left(r^2\frac{\partial \Psi}{\partial r}\right) + \frac{1}{r^2 \sin\theta}\frac{\partial}{\partial \theta}\left(\sin\theta\frac{\partial \Psi}{\partial \theta}\right) = 4\pi G\rho. \tag{3}$$

Here, ρ, p, V_ϕ, B_ϕ and Ψ denote the gas density, pressure, toroidal velocity component, toroidal magnetic field and gravitational potential, respectively. Also, G and M are the gravitational constant and the mass of the central star, respectively. The solution of equations (1)–(3), in general, is a difficult task. Therefore, to simplify the problem, we impose two constraints. We adopt for B_ϕ and V_ϕ the same form as that given in Banerjee et al. (1995). They assume that the magnetic field of the central star is dipolar

$$B_r = 2B_0\left(\frac{R}{r}\right)^3 \cos\theta, \tag{4}$$

$$B_\theta = B_0\left(\frac{R}{r}\right)^3 \sin\theta, \tag{5}$$

where B_0 is the magnetic field strength on the surface of the central star near the pole and R is its radius. They showed that the dipolar field with the azimuthal motion of the gas disc could make a toroidal component of the magnetic field, i.e.

$$B_\phi = B_1\left(\frac{r}{R}\right)^{(k-(3/2))} \sin^{-2k}\theta, \tag{6}$$

where B_1 is an arbitrary constant with the dimension of a magnetic field strength, and $k \leqslant 3/2$ is a real constant. The general solution for V_ϕ is

$$V_\phi = V_0\left(\frac{r}{R}\right)^{[n+(3/2)]} \sin^{-2n}\theta, \tag{7}$$

where R denotes the radius of the star. V_0 is a constant with the dimension of a velocity and n is a real constant.

Now, we try to solve our equations with these constraints. At first we introduce x according to

$$x = \frac{r}{R_\mathrm{d}}, \qquad \alpha = \frac{R_\mathrm{d}}{R}, \tag{8}$$

where R and R_d are the star and the disc radii, respectively. Now we rewrite equations (6) and (7) as

$$B_\phi = B_1 \alpha^{k-(3/2)} x^{k-(3/2)} \sin^{-2k}\theta, \tag{9}$$

$$V_\phi = V_0 \alpha^{n+(3/2)} x^{n+(3/2)} \sin^{-2n}\theta, \tag{10}$$

where B_1 and V_0 are the strength of the toroidal component of the magnetic field and the rotational velocity on the surface of the star, respectively. We can see clearly that the structure of the magnetic field of the central star can be modified by a rotational velocity of the gas disc.

2.1 Magnetic field configuration

In this subsection we want to study the magnetic field of central stars in the presence of a rotating gas disc. In a magnetized disc, magnetic field lines are deformed by the rotating gas. In this case, the gas is expected to be tied to the magnetic field lines and its inertia causes them to be bent backward and to create a toroidal component.

To study the magnetic field configuration within the disc we will look at the magnetic field lines, which satisfy the following equation:

$$\frac{\mathrm{d}r}{B_r} = \frac{r\,\mathrm{d}\theta}{B_\theta} = \frac{r\sin\theta\,\mathrm{d}\phi}{B_\phi}. \tag{11}$$

In order to visualize the field line configurations, we now choose $k = -(3/2)$ in equation (6). It is useful to express the results in a Cartesian frame through the usual relations ($X = r\sin\theta\cos\phi$, $Y = r\sin\theta\sin\phi$, $Z = r\cos\theta$). If we apply these transformations to the force equation we can obtain the corresponding parametric equations that generate the magnetic field configurations:

$$X = r_{\rm in}\cos\left[\phi_0 - \beta\left(\frac{r_{\rm in}}{R}\right)^3\cos\theta\right]\sin^3\theta, \tag{12}$$

$$Y = r_{\rm in}\sin\left[\phi_0 - \beta\left(\frac{r_{\rm in}}{R}\right)^3\cos\theta\right]\sin^3\theta, \tag{13}$$

$$Z = r_{\rm in}\sin^2\theta\cos\theta. \tag{14}$$

Here, Φ_0 is a constant of integration (because we consider axisymmetric solutions, we can set it to zero without any loss of generality), $\beta = B_1/B_0$ and $r_{\rm in}$ is the disc inner radius. From the above equations we can see that the azimuthal component of the magnetic field can affect magnetic field line configurations in the disc. In Fig. 1 we plot several two-dimensional (2D) field line configurations. We can see that when the toroidal component of the magnetic field is larger, the deformation of the magnetic field line is more obvious. In Fig. 2 we plot several three-dimensional (3D) magnetic field configurations with the same parameters.

Now we return to equations (1)–(3) and introduce other dimensionless variables for the gravitational potential, the density and the pressure of the disc's material:

$$S = \frac{\Psi}{\Psi_0}, \qquad \Sigma = \frac{\rho}{\rho_0}, \qquad \Lambda = \frac{p}{p_0}. \tag{15}$$

Here, Ψ_0, ρ_0 and P_0 are defined as

$$\Psi_0 = \frac{GM}{R_{\rm d}} \tag{16}$$

$$\rho_0 = \rho\left(r = R_{\rm d}, \theta = \frac{\pi}{2}\right), \tag{17}$$

$$p_0 = p\left(r = R_{\rm d}, \theta = \frac{\pi}{2}\right). \tag{18}$$

By inserting these dimensionless parameters into equations (1) and (2), and by performing some simplifications, we obtain

$$\begin{aligned}\frac{\partial S}{\partial x} &= -C_B\frac{x^{2k-4}}{\Sigma}\left(k-\frac{1}{2}\right)\sin^{-4k}\theta + C_{\rm c}x^{2n+2}\sin^{-4n}\theta \\ &\quad -C_{\rm t}\frac{1}{\Sigma}\frac{\partial\Lambda}{\partial x} - \frac{1}{x^2},\end{aligned} \tag{19}$$

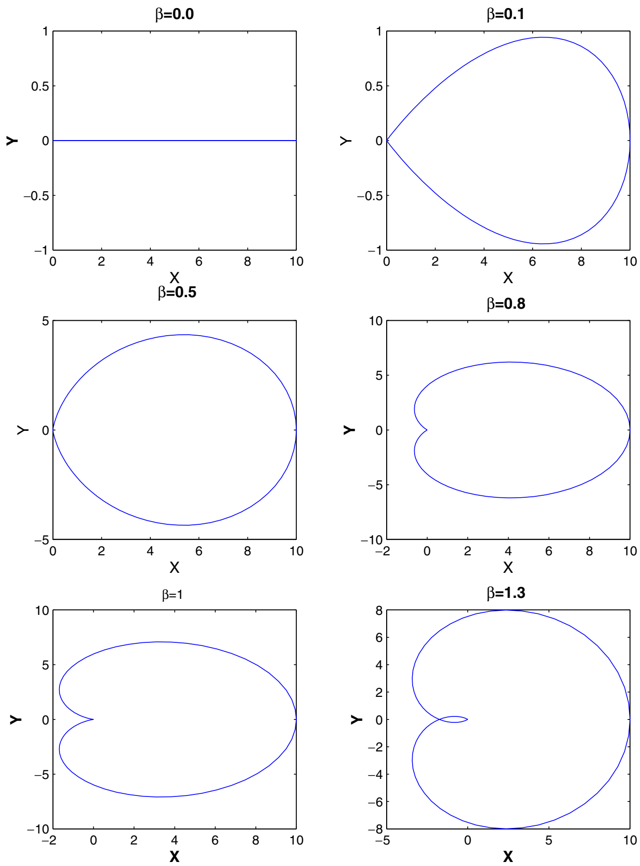

Figure 1. The 2D magnetic field configurations in an X–Y plane as a function of θ, which runs from $\theta_{\rm min} = 0$ to $\theta_{\rm max} = \pi$, at $r = r_{\rm in} = 10$ and $R = 7$ for different values of $\beta = B_1/B_0$.

$$\begin{aligned}\frac{\partial S}{\partial\theta} &= -C_B\frac{x^{2k-3}}{\Sigma}(-2k+1)\sin^{-4k+1}\theta\cos\theta \\ &\quad + C_{\rm c}x^{2n+3}\sin^{-4n}\theta\cot\theta - C_{\rm t}\frac{1}{\Sigma}\frac{\partial\Lambda}{\partial\theta},\end{aligned} \tag{20}$$

where C_B, $C_{\rm c}$ and $C_{\rm t}$ are constants defined by

$$C_B = \frac{(B_1^2/4\pi\rho_0)}{(GM/R_{\rm d})}\alpha^{2k-3}, \tag{21}$$

$$C_{\rm c} = \frac{V_0^2}{(GM/R_{\rm d})}\alpha^{2n+3}, \tag{22}$$

$$C_{\rm t} = \frac{(P_0/\rho_0)}{(GM/R_{\rm d})}. \tag{23}$$

By introducing three dimensionless parameters indicating the relative importance of the energy of the toroidal component of the magnetic field (C_B), the centrifugal energy ($C_{\rm c}$) and the thermal energy ($C_{\rm t}$) with respect to the gravitational potential energy of the central object, we can study them separately. If this simplification is used for the Poisson equation (equation 3), we find that

$$\frac{1}{x^2}\frac{\partial}{\partial x}\left(x^2\frac{\partial S}{\partial x}\right) + \frac{1}{x^2\sin\theta}\frac{\partial}{\partial\theta}\left(\sin\theta\frac{\partial S}{\partial\theta}\right) = \frac{3M_{\rm d}}{M}\Sigma, \tag{24}$$

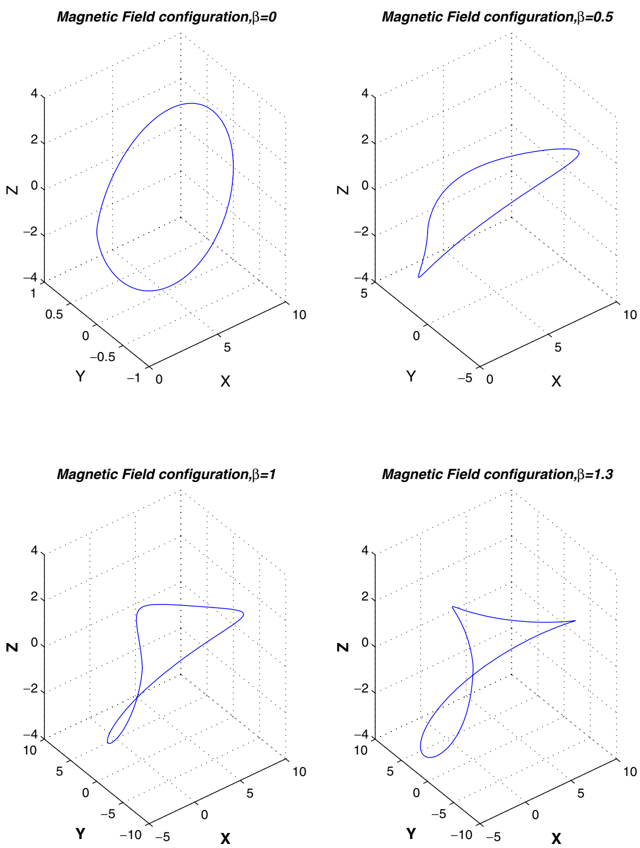

Figure 2. The 3D magnetic field configurations as a function of θ, which runs from $\theta_{\min} = 0$ to $\theta_{\max} = \pi$, at $r = r_{\rm in} = 10$ and $R = 7$ for different values of $\beta = B_1/B_0$.

where $M_{\rm d}$ is the mass of the disc out to $R_{\rm d}$

$$M_{\rm d} = \frac{4\pi}{3} R_{\rm d}^3 \rho_0. \tag{25}$$

We may introduce another dimensionless variable $C_{\rm g}$ which gives the importance of self-gravity. $C_{\rm g}$ is the ratio of the disc mass to the central object mass:

$$C_{\rm g} = \frac{3M_{\rm d}}{M}. \tag{26}$$

We would like to investigate self-similar solutions that describe the equilibrium structure of the thick disc. Thus, we introduce self-similar solutions for the density and pressure of the gas disc:

$$\Sigma(r, \theta) = \frac{D(\theta)}{x^{\epsilon}} \tag{27}$$

$$\Lambda(r, \theta) = \frac{P(\theta)}{x^{\delta}}. \tag{28}$$

Because we do not consider energy transport mechanisms, no specific form for the equation of state is assumed. As a result of our model we find that the density and pressure clearly show no polytropic, isothermal or other simple relation. We show that the indices in the non-self-gravitating and self-gravitating cases are completely different and that the mass distribution of the disc changes due to this fact. Solving equations (19) and (20) and equations (27) and (28) gives ϵ and δ.

3 NON-SELF-GRAVITATING SOLUTION

In this section we try to derive a self-similar solution of non-self-gravitating discs. In this regime we put S equal to zero. If we put equations (27) and (28) into equations (19) and (20) we obtain

$$-\left(k - \frac{1}{2}\right) C_B x^{2k-4+\epsilon} \frac{\sin^{-4k}\theta}{D} + C_{\rm c} x^{2n+2} \sin^{-4n}\theta + \delta C_{\rm t} x^{\epsilon-\delta-1} \frac{P}{D} - \frac{1}{x^2} = 0 \tag{29}$$

$$(2k-1) C_B x^{2k-3+\epsilon} \frac{\sin^{-4k-1}\theta \cos\theta}{D} + C_{\rm c} x^{2n+3} \sin^{-4n}\theta \times \cot\theta - C_{\rm t} x^{\epsilon-\delta} \frac{1}{D}\frac{{\rm d}P}{{\rm d}\theta} = 0. \tag{30}$$

In order to obtain the indices of the self-similar solution, we require that, in each equation, the exponent of x be the same for all the terms. Here we obtain

$$2k - 4 + \epsilon = 2n + 2 = \epsilon - \delta - 1 = -2, \tag{31}$$

and we have

$$\epsilon = 2 - 2k \tag{32}$$

$$n = -2 \tag{33}$$

$$\delta = -2k + 3. \tag{34}$$

These equations state that, for obtaining a physical solution, k must be less than unity. Then by putting the self-similar indices in the equations and by performing some simplifications, we obtain

$$-\left(k - \frac{1}{2}\right) C_B \frac{\sin^{-4k}\theta}{D} + C_{\rm c} \sin^8\theta + (3 - 2k) C_{\rm t} \frac{P}{D} - 1 = 0 \tag{35}$$

$$(2k-1) C_B \frac{\sin^{-4k-1}\theta\cos\theta}{D} + C_{\rm c}\sin^8\theta\cot\theta - C_{\rm t}\frac{1}{D}\frac{{\rm d}P}{{\rm d}\theta} = 0. \tag{36}$$

We have two equations with two unknowns. The first equation can be used to express P as a function of D:

$$P(\theta) = \frac{1}{(3-2k)C_{\rm t}} \times \left[(1 - C_{\rm c}\sin^8\theta) D(\theta) + \left(k - \frac{1}{2}\right) C_B \sin^{-4k}\theta\right]. \tag{37}$$

With our definitions of ρ_0 and P_0, we have $D(\theta = \pi/2) = 1$ and $P(\theta = \pi/2) = 1$. If we introduce this boundary condition in equation (37), $C_{\rm t}$ can be calculated:

$$C_{\rm t} = \frac{1}{(3-2k)}\left[1 - C_{\rm c} + \left(k - \frac{1}{2}\right) C_B\right]. \tag{38}$$

Now if we introduce equation (37) into equation (36), we find

$$\frac{{\rm d}D}{{\rm d}\theta} = g(\theta) D + f(\theta), \tag{39}$$

where

$$g(\theta) = (11 - 2k)\frac{C_{\rm c}\sin^7\theta\cos\theta}{1 - C_{\rm c}\sin^8\theta}, \tag{40}$$

$$f(\theta) = 3(2k-1)C_B \frac{\sin^{-4k-1}\theta\cos\theta}{1 - C_c\sin^8\theta}. \tag{41}$$

For this equation we perform the following change of variable:

$$D(\theta) = [1 - C_c\sin^8\theta]^{-[(11-2k)/8]} D_1(\theta), \tag{42}$$

$$\frac{dD_1(\theta)}{d\theta} = [1 - C_c\sin^8\theta]^{(11-2k)/8} f(\theta), \tag{43}$$

or

$$\frac{dD_1(\theta)}{d\theta} = 3C_B(2k-1)[1-C_c\sin^8\theta]^{(3-2k)/8}\sin^{-4k-1}\theta\cos\theta. \tag{44}$$

The solution of this equation can be written as

$$D_1(\theta) = 3C_B(2k-1)I(\theta) + D_{01}, \tag{45}$$

where

$$I(\theta) = \int_0^{\theta} [1 - C_c\sin^8\theta']^{(3-2k)/8}\sin^{-4k-1}\theta'\cos\theta' d\theta'. \tag{46}$$

Now we return to our boundary conditions for the density. The maximum density is at $\theta = \pi/2$ where $D(\pi/2) = 1$. Now we can find the value of D_{01} as

$$\begin{aligned} D_1\left(\frac{\pi}{2}\right) &= [1 - C_c\sin^8\theta]^{(11-2k)/8}|_{\theta=\pi/2} D\left(\frac{\pi}{2}\right) \\ &= [1 - C_c]^{(11-2k)/8} \end{aligned}. \tag{47}$$

Thus

$$D_{01} = [1 - C_c]^{(11-2k)/8} - 3C_B(2k-1)I\left(\theta = \frac{\pi}{2}\right). \tag{48}$$

Hence we can find the density distribution:

$$D(\theta) = \left\{(1 - C_c)^{(11-2k)/8} - 3C_B(2k-1)\left[I\left(\frac{\pi}{2}\right) - I(\theta)\right]\right\} \times [1 - C_c\sin^8\theta]^{-[(11-2k)/8]}. \tag{49}$$

The important result from this equation is that the value of the density is not zero in the rotation axis. This value depends on our dimensionless parameters, C_B and C_c, where C_B represents the effect of the toroidal component of the magnetic field and C_c represents the effect of the rotation velocity.

Fig. 3 shows typical examples of the self-similar solution in equations (37) and (49). In Fig. 3, the density profiles, the isodensity contours and the variations of pressure along the meridional axes are represented. The density profiles for different values of C_c (rotational velocity) and k are displayed. As can be seen, the parameter C_c determines the overall shape of the matter distribution. By increasing the effect of the rotational velocity (C_c), the shape of the disc changes to a thinner one, which is due to centrifugal force. In Fig. 3, we also present the isodensity contours for the same value of C_c. As can be seen, the shape of the disc is strongly modified for different values of C_c. We can see that, in this case, the density does not vanish at $\theta = 0, \pi$ (in the rotational axes). Our solution agrees with (Banerjee et al. 1995) solutions for such systems.

We should mention that the solution we have found is a mathematical one. As a result, the solution has a physical meaning only for parts of the parameter space. In this self-similar solution, we have a singularity in $\theta = 0, \pi$ that arises from $\sin\theta$ in the integral of equation (46). Thus, we cannot study the effect of the magnetic field in the equilibrium structure of the gas disc. That is the nature of the solution. After we have found the analytical solution for non-self-gravitating discs, we will try to investigate the effect of self-gravity in such discs.

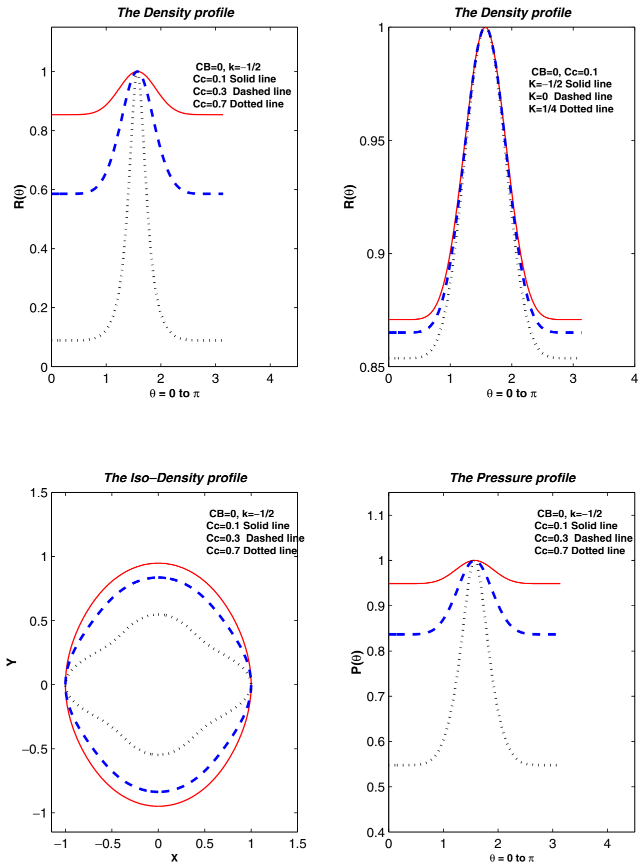

Figure 3. Variation of density along the meridional as a function of θ from $\theta_{min} = 0$ to $\theta_{max} = \pi$: top left, for different values of C_c (rotational velocity); top right, for different values of k. Bottom left: Isodensity contour for different values of C_c. Bottom right: Variation of pressure with different values of C_c.

4 SELF-GRAVITATING SOLUTION

In order to gain a better understanding of the physical situation of the disc, we include self-gravity in the above equations. The self-similar technique is utilized once again. If we introduce equations (27) and (28) into equations (19) and (20) we obtain

$$\frac{\partial S}{\partial x} = -C_B\left(k - \frac{1}{2}\right)x^{2k-4+\epsilon}\frac{\sin^{-4k}\theta}{D(\theta)} + C_c x^{2n+2}\sin^{-4n}\theta + \delta C_t x^{\epsilon-\delta-1}\frac{P(\theta)}{D(\theta)} - \frac{1}{x^2}, \tag{50}$$

$$\frac{\partial S}{\partial \theta} = -C_B(-2k+1)x^{2k-3+\epsilon}\frac{\sin^{-4k-1}\theta\cos\theta}{D(\theta)} + C_c x^{2n+3}\sin^{-4n}\theta\cot\theta - C_t x^{\epsilon-\delta}\frac{1}{D(\theta)}\frac{dP(\theta)}{d\theta}. \tag{51}$$

In order to find the self-similar solution, we must set equal the terms that have the same power. We obtain

$$\epsilon = \frac{5-2k}{2} \tag{52}$$

$$n = \frac{2k - 7}{4} \tag{53}$$

$$\delta = 3 - 2k. \tag{54}$$

Now we can identify the radial dependence of the density and pressure of the gas disc (ϵ and δ) as functions of k. We can insert equations (50) and (51) into equation (24) and using equation (27) we can find

$$\frac{\partial S}{\partial x} = H(\theta) x^{(2k-3)/2} - \frac{1}{x^2}, \tag{55}$$

$$\frac{\partial S}{\partial \theta} = W(\theta) x^{(2k-1)/2}, \tag{56}$$

where we have used k as a free parameter and

$$H(\theta) = \left[-\left(k - \frac{1}{2}\right) C_B \frac{\sin^{-4k}\theta}{D(\theta)} + C_c \sin^{-2k+7}\theta + (3 - 2k) C_t \frac{P(\theta)}{D(\theta)} \right], \tag{57}$$

$$W(\theta) = \left[C_B(-2k + 1) \frac{\sin^{-4k-1}\theta \cos\theta}{D(\theta)} + C_c \sin^{-2k+7} \times \theta \cot\theta - C_t \frac{1}{D(\theta)} \frac{\mathrm{d}P}{\mathrm{d}\theta} \right]. \tag{58}$$

Now if we introduce equations (55) and (56) into equation (24) and do some simplifications, we obtain an ordinary differential equation with two unknown functions ($D(\theta)$ and $P(\theta)$):

$$\left(\frac{2k + 1}{2}\right) H(\theta) + \frac{1}{\sin\theta} \frac{\mathrm{d}}{\mathrm{d}\theta} [\sin\theta W(\theta)] = \frac{3M_\mathrm{d}}{M} D(\theta). \tag{59}$$

In order to solve this equation, we need another relation between $D(\theta)$ and $P(\theta)$. By looking at the definitions of H and W, we can find

$$\frac{2}{2k - 1} \frac{\mathrm{d}H}{\mathrm{d}\theta} = W(\theta). \tag{60}$$

Now by solving equations (59) and (60) we can find the angular dependence of the density and pressure of the gas disc (D, P). We linearize these equations, introduce another dimensionless constant defined as the ratio of the disc mass to the mass of the central object (C_g), and we use $Q = 1/D$ instead of D in order to simplify the equations. Thus, with some calculations, we obtain

$$\frac{\mathrm{d}y_1}{\mathrm{d}\theta} = S(\theta, y_1, y_2, y_3), \tag{61}$$

$$\frac{\mathrm{d}y_2}{\mathrm{d}\theta} = y_3, \tag{62}$$

$$\frac{\mathrm{d}y_3}{\mathrm{d}\theta} = T(\theta, y_1, y_2, y_3), \tag{63}$$

where $y_1 = Q = 1/D$, $y_2 = P$, $y_3 = \mathrm{d}P/\mathrm{d}\theta$, and S and T are complex functions of θ, y_1, y_2 and y_3. We solve these linear equations, with two point boundary conditions with the shooting method. Solving these equations gives the meridional component of the density and pressure. We used the boundary conditions of Narayan & Yi (1995):

$$\frac{\mathrm{d}\rho}{\mathrm{d}\theta}\Big|_{\theta=0} = \frac{\mathrm{d}\rho}{\mathrm{d}\theta}\Big|_{\theta=\pi/2} = 0 \tag{64}$$

$$\frac{\mathrm{d}p}{\mathrm{d}\theta}\Big|_{\theta=0} = \frac{\mathrm{d}p}{\mathrm{d}\theta}\Big|_{\theta=\pi/2} = 0. \tag{65}$$

By changing the value of the dimensionless parameters C_B, C_c, C_t and C_g, we can study the influence of the toroidal magnetic field, toroidal velocity, thermal energy and self-gravity of the gas disc on its own equilibrium structure. In Figs 4–6 we plot some of our results. By comparing the results in Figs 4 and 5, which are calculated for different values of C_g, we can see how the disc is more sensitive to the influence of self-gravity. Fig. 4 shows the variations of the density for different values of C_g, C_B and C_c in the meridional direction. Concerning the geometrical shape of the disc we can see the tendency of the disc to become thinner when self-gravity plays an important role (C_g is large). Then, we can see that a strong magnetic field coming from the central star can produce a large toroidal component, which can change the thickness of the disc near the pole. Fig. 4 shows the isodensity contours of the disc for different values of C_g and C_B. In Fig. 6 we present the isodensity profile of the disc for different values of C_c and the iso-pressure profile of the disc for different values of C_B. We can see in the iso-pressure profile that near the pole there is a singularity; perhaps

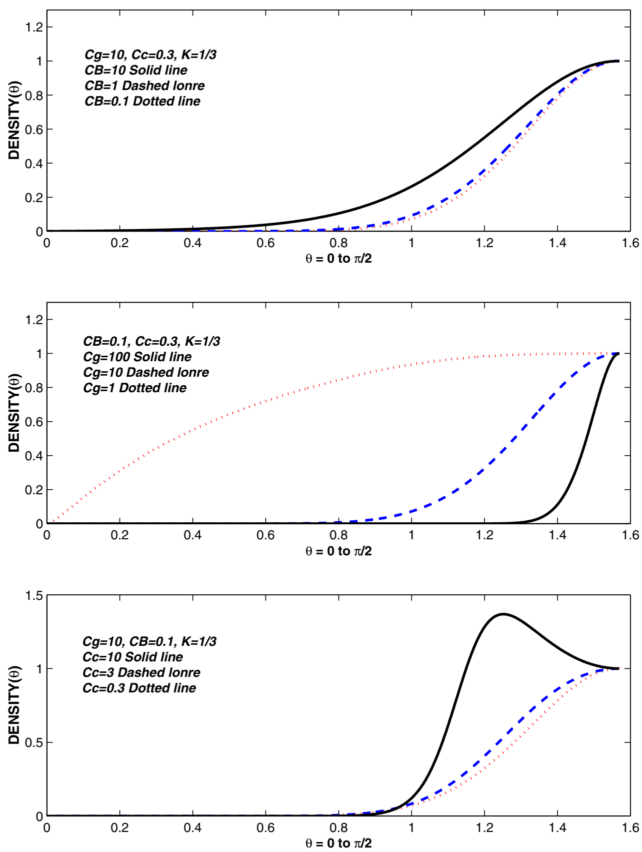

Figure 4. Variation of the density of the disc for several values of the parameters: top, for different values of C_B that represents the importance of the magnetic field; middle, for different values of C_g that represents the importance of self-gravity; bottom, for different values of C_c which represents the importance of the rotational velocity.

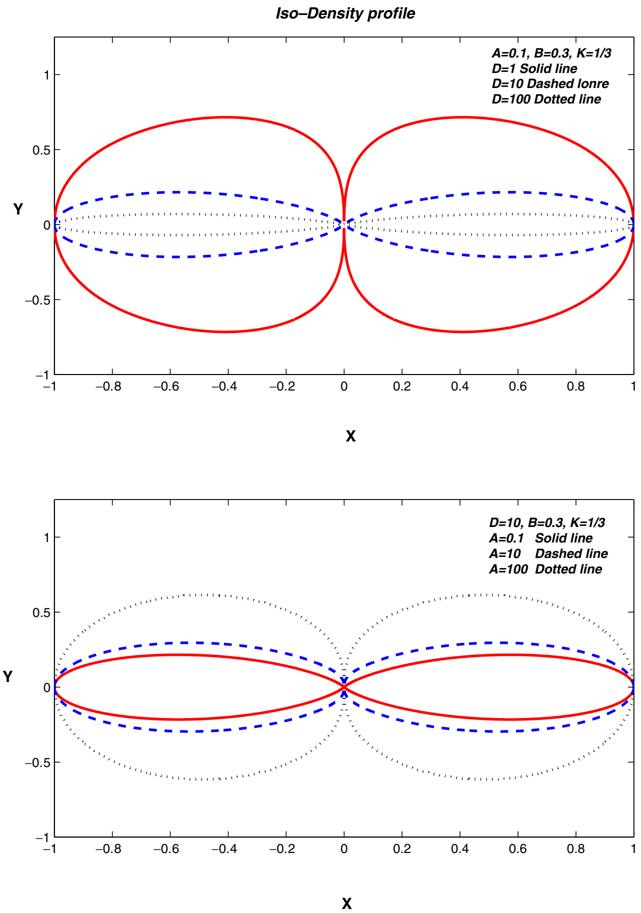

Figure 5. Isodensity contours of the self-gravitating discs: top, for different values of C_g that represents the importance of self-gravitation; bottom, for different values of C_B which represents the importance of the magnetic energy.

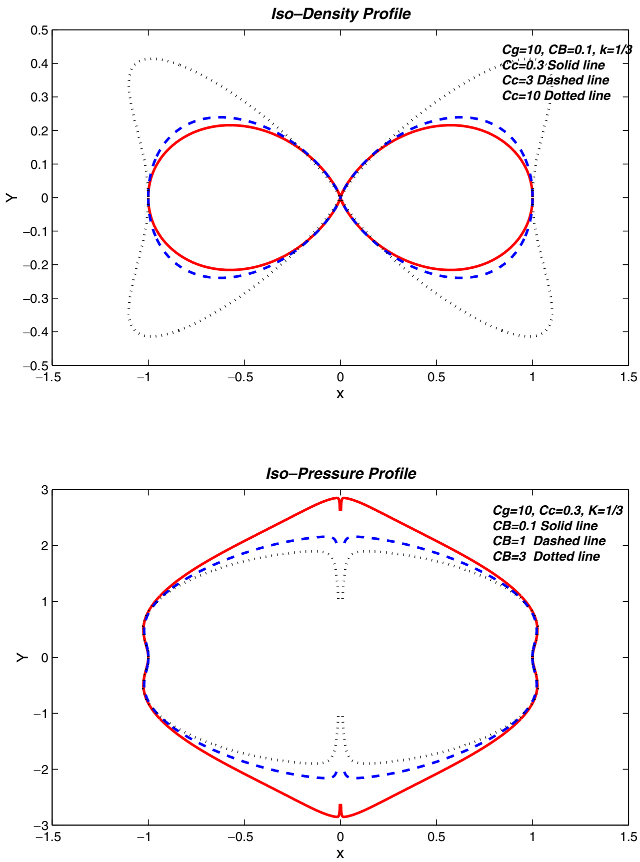

Figure 6. Isodensity contours of the self-gravitating accretion discs: top, for different values of C_c, which represents the importance of rotational velocity; bottom, iso-pressure contours of the disc for different values of C_B, which represents the importance of the magnetic field.

this large pressure gradient could produce a jet from the pole. In order to test this effect we should investigate the time evolution of such systems. This could be the subject of future works.

Concerning the ratio of the mass of the disc to the mass of the central star, Eriguchi & Muller (1993) extended their code to include a central object for a thick disc and calculated the equilibrium structure of the disc which rotates according to the j-const law, where j is the specific angular momentum. Comparing this with the toroidal star of Hashimoto et al. (1993), where the central object is not included, the relative thickness of the disc is smaller, which is caused by effects due to gravity of the central star (see figures in Eriguchi & Muller 1993). As for the rotation law, Hashimoto et al. (1993) and Eriguchi & Muller (1993) obtained rather thick discs, while Hashimoto et al. (1995) found a flat disc shape where the gravitational force of the central object becomes relatively weak compared with the self-gravity of the disc. Our results agree with the latter. We can see in Figs 4–6 that the shape of the disc (or disc thickness) is influenced by the rotational law and the ratio of the disc mass to the mass of the central star.

5 DISCUSSION AND CONCLUSIONS

In this paper, we find a global equilibrium of a self-gravitating disc around a magnetized compact object. We ignore the effects of energy dissipation and radial flow. We have investigated a stationary model for a self-gravitating disc influenced by a strong magnetic field coming from the central object. We ignore the effects of the local magnetic field of the disc. We consider that the radial flow is negligible with respect to the azimuthal motion of the gas in the disc. We find two types of self-similar solutions for such discs. The first is the non-self-gravitating self-similar solution that shows that the shape of the disc changes when the physical parameters are modified. The second is the self-gravitating self-similar solution. In this class of solutions we can study the effect of self-gravity on the shape and thickness of the disc.

In the non-self-gravitating solution, we find an analytical solution for some parts of the parameter space. This solution is found with a self-similarity method, and it gives a picture of the equilibrium structure of the gas material around a magnetized compact object. The solution shows that the rotational velocity of the gas disc can change the equilibrium picture. The important result that can be inferred from this solution is the non-vanishing value of the density on the rotation axis. This value depends on the dimensionless parameters, C_B and C_c, where C_B represents the effect of the magnetic field and C_c represents the effect of the rotational velocity.

In the self-gravitating solution, we find the vertical (meridional) dependence of the gas density in the disc (Fig. 4). The external dipole field can change the thickness of the disc near the pole, and the existence of a sharp density gradient in the θ-direction indicates a rapid decrease of the matter density away from the equatorial plane. However, when self-gravity plays an important role in the disc equilibrium (by increasing C_g) we can see that the thickness of the disc decreases.

In Figs 5 and 6 we show some isodensity and iso-pressure contours of the equilibrium configuration of the disc for different values of C_B, C_c, C_g and k. In the iso-pressure profile we can see a large pressure gradient near the poles, which may lead to outflows in those regions. This idea would require further study, such as a dynamical investigation.

We see that the presence of self-gravity in a thick disc can change the geometrical shape of the disc and plays an important role in equilibrium structure of the disc. We also see that the strength of the magnetic field can change the structure of the disc near the poles. Finally, we must admit that our model does not deserve the name 'accretion' disc, because we did not include the accretion (mass) flow.

This study, one of the first of its kind, is a search for an equilibrium structure of a thick disc in the presence of an external stellar dipole along with a self-consistently generated toroidal magnetic field B_ϕ. The meridional structure of the disc is mainly due to the balance of the plasma pressure gradient, magnetic force due to B_ϕ and centrifugal force. The existence of an equilibrium structure, in fact, encourages one to look for generalizations of the analysis to the case when the radial velocity $V_r \neq 0$, representing accretions. On the other hand, yet another important aspect to be considered is the generalization of the Newtonian analysis to general relativistic formalism wherein space–time curvature produced by the strong gravitational field of the central object would modify the magnetic fields and introduce new features.

Our disc model might also apply to systems where the central object is a black hole, a neutron star or an active galactic nucleus. However, in this paper we have modelled the disc under the assumption of a Newtonian potential. For a system where the central object is a black hole, the pseudo-Newtonian potential will play an essential role near the central object. The modification arising from a pseudo-Newtonian potential to the disc will be investigated in a future paper. Consequently, we cannot calculate the accretion luminosity. Thus, to compare our results with other models or observations, it will be necessary to include mass flow in our model.

ACKNOWLEDGMENTS

We are grateful to the referee for a very careful reading of the manuscript and for suggestions which have helped us to improve the presentation of our results. We are grateful to Mohsen Shadmehri for continuous encouragement and useful discussions. We thank Kattia Ferriere, Daniel Reese and Saeed Farivar for their useful comments.

REFERENCES

Banerjee D., Bhatt J. R., Das A. C., Prasanna A. R., 1995, ApJ, 449, 789
Blandford R. D., Znajek R. L., 1977, MNRAS, 179, 433
Bodo G., Curir A., 1992, A&A, 253, 318
Cassen P., Moosman A., 1981, Icarus, 48, 353
Eriguchi Y., Müller E., 1993, ApJ, 416, 666
Frank J., King A., Raine D., 1992, Accretion Power in Astrophysics. Cambridge Univ. Press, Cambridge
Fukue J., Sakamoto C., 1992, PASJ, 44, 553
Hachisu I., 1986a, ApJS, 61, 479
Hachisu I., 1986b, ApJS, 62, 461
Hashimoto M., Tohline J. E., Eriguchi Y., 1987, ApJ, 323, 592
Hashimoto M., Eriguchi Y., Arai K., Muller E., 1993, A&A, 268, 131
Hashimoto M., Eriguchi Y., Muller E., 1995, A&A, 297, 135
Lovelace R. V. E., Mehanian C., Mobarry C. M., Sulkanen M. E., 1986, ApJS, 62, 1
Lubow S. H., Papaloizou J. C. B., Pringle J. E., 1994, MNRAS, 267, 235
Lynden-Bell D., Pringle J. E., 1974, MNRAS, 168, 603
Mobarry C. M., Lovelace R. V. E., 1986, ApJ, 309, 455
Narayan R., Yi I., 1995, ApJ, 444, 231
Paczynski B., 1978, Acta Astron., 28, 91
Pen U.-L., 1994, ApJ, 429, 759
Pringle J. E., 1981, ARA&A, 19, 137
Shakura N. I., Sunyaev R. A., 1973, A&A, 24, 337
Tomley L., Cassen P., Steiman-Cameron T., 1991, ApJ, 382, 530
Tripathy S. C., Prasanna A. R., Das A. C., 1990, MNRAS, 246, 384
Woodward W., Sankaran S., Tohline J. E., 1992, ApJ, 394, 248

This paper has been typeset from a TEX/LATEX file prepared by the author.